

# Reflectivity of hexagonal ice crystals

D.N. Romashov

*Institute of Atmospheric Optics,  
Siberian Branch of the Russian Academy of Sciences, Tomsk*

Received July 15, 1999

The paper presents a study of the influence of orientation of the hexagonal water ice crystals on the intensity of backscattering from an unpolarized incident radiation. A detailed physical analysis of the processes of formation of the beams mostly contributing into the backscattering is presented.

The elements of the backscattering phase matrix (BSPM) of hexagonal crystals were calculated in Ref. 1 using the method of beam splitting (MBS). It was shown that the highest intensity of backscattering is observed when the radiation is incident along the crystal axis or perpendicular to one of four quadrangular sides. These peaks are very narrow due to large size of a crystal, so the dependence of the intensity of backscattering on other orientations plays significant role in calculation of the intensity averaged over the ensemble of particles. This paper presents detailed physical description of the influence of crystal orientation on the intensity of backscattering from unpolarized incident radiation.

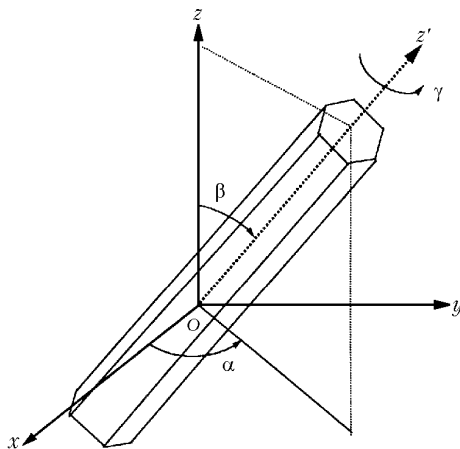


**Fig. 1.** Geometry of scattering on an arbitrary oriented hexagonal crystal.

The size of a hexagonal crystal is determined by the following parameters:  $L$  is the length along the crystal axis,  $a$  is the radius of the circle circumscribed around the hexagonal basis. Orientation of the crystal relative to the incident radiation is defined by three Euler angles  $\alpha$ ,  $\beta$ , and  $\gamma$  (Fig. 1),  $\beta$  is the angle between the incident radiation direction and the crystal axis,  $\alpha$  is the angle between the reference plane and the plane containing the axis of the incident radiation beam and the crystal axis, and  $\gamma$  is the angle of rotation about the crystal axis. In what follows below we

always perform averaging over the angle  $\gamma$  with the probability density  $3/\pi$ :

$$\mathbf{M}(\alpha, \beta) = \frac{3}{\pi} \int_0^{\pi/3} \mathbf{M}'(\alpha, \beta, \gamma) d\gamma,$$

where  $\mathbf{M}'(\alpha, \beta, \gamma)$  is the BSPM of an arbitrary oriented hexagonal crystal. At  $\gamma = 0$  one of the sides of the crystal is perpendicular to the plane containing the axis of the incident radiation beam and the crystal axis. It was shown<sup>1</sup> that in the case of backscattering one can restrict oneself to the orientations  $\alpha = 0$  without any loss of information. It was also revealed<sup>1</sup> that the behavior of  $M_{11}(0, \beta)$  element as a function of  $\beta$  is principally determined by the hexagonal crystals with the orientation at  $\gamma = 0$  ( $\beta \neq 0$ ).

The dependence  $M_{11}(0, \beta)$  for thin hexagonal plates ( $\beta \neq 0; 90^\circ$ ) calculated without the account of interference by MBS<sup>1</sup> is shown in Fig. 2.

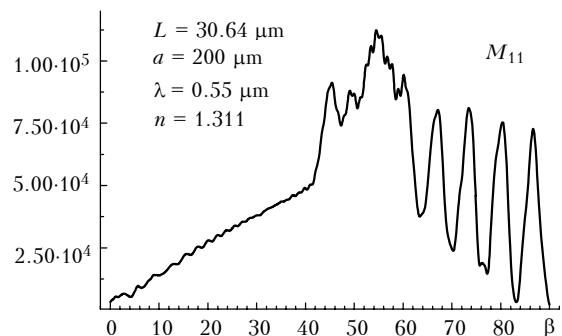


**Fig. 2.** The dependence of  $M_{11}(0, \beta)$  on the angle  $\beta$  for an ensemble of hexagonal plates oriented uniformly about the axis.

To explain such a complicated behavior of  $M_{11}(0, \beta)$  as a function of  $\beta$ , let us carry out detailed analysis of the process of the beam formation using as an example the hexagonal plates with  $\gamma = 0$ . The plate cross sections passing through its axis and the normals to two opposite quadrangular sides  $G_1$  and  $G_2$  are shown in Figs. 3–5. The boundaries of the formed beams are shown by solid arrows. To imagine the process of the beam formation in Figs. 3–5, it is sufficient to follow

the trace of an arbitrary beam between the boundary beams (dotted arrows in Fig. 3). The beams outgoing along the backward direction are of two types: (a) the beams going out from the hexagonal basis  $O_1$  (see Fig. 3); and (b) the beams going out from the side  $G_1$  (see Fig. 4).

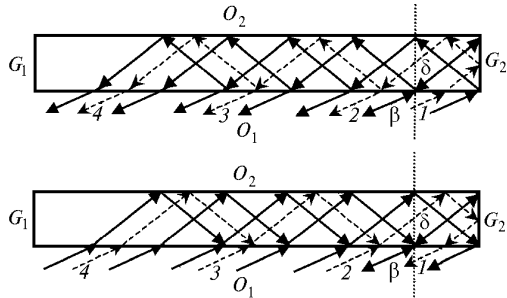


**Fig. 3.** The diagrams of formation of beams in the hexagonal plates with  $\gamma = 0$ , which are outgoing from the plate bases and make the greatest contribution to the backscattering at a slant incidence of radiation.

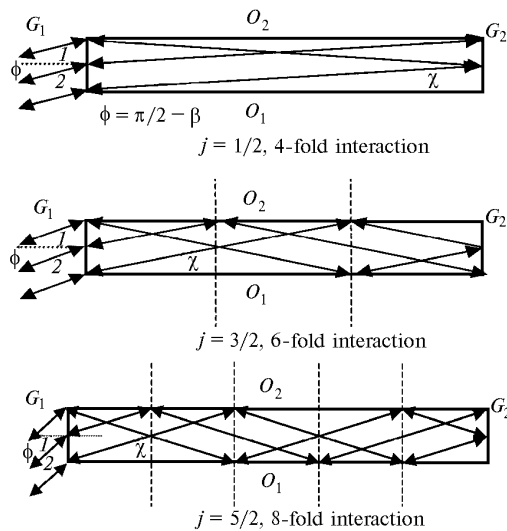


**Fig. 4.** The diagrams of formation of beams in the hexagonal plates with  $\gamma = 0$ , which are outgoing from the side and give the greatest contribution to the backscattering at a slant incidence of radiation.

Only the beams "a" of 4-, 6-, and 8-fold interaction are shown in Fig. 3, however, it is clear that the beams of greater multiplicity can be formed at certain values of  $\beta$ ,  $a$ , and  $L$ . The beam 1 in the upper part of Fig. 3 is incoming, beams 2, 3, and 4 are outgoing, and the beams 2, 3, and 4 in the lower part are incoming, and the beam 1 is outgoing. It is seen that the beams 1 and 2 in Fig. 3 are mutually inverse for 4-fold processes of the formation of beams outgoing from the bases  $O_1$ , 1 and 3 are inverse for the 6-fold processes, and 1 and 4 are inverse for the 8-fold processes. The total area of the cross section of two such beams is expressed through the parameters  $\beta$ ,  $a$ , and  $L$  as follows:

$$S_a(\beta, a, L) = \frac{2aL \cos\beta \sin\beta}{\sqrt{n^2 - \sin^2\beta}}, \quad (1)$$

where  $n$  is the relative refractive index.

Since no total internal reflection on the bases  $O_1$  and  $O_2$  occurs for the beams "a," it is sufficient for further analysis to restrict oneself to the consideration of the 4-fold beams "a." It is a characteristic peculiarity of the beams "a" that their contribution is significant at the values  $\beta$  from 0 to  $58^\circ$ , because the total internal reflection on the side  $G_2$  takes place in this case.

Quite different pattern is observed for the beams "b," because the total internal reflection on the bases  $O_1$  and  $O_2$  takes place at  $\beta > 32^\circ$ , and so one cannot ignore the beams of higher multiplicity. Three processes are shown in Fig. 4, when all beams incident on the side  $G_1$  are outgoing through  $G_1$  backwards as a result of the total internal reflection, i.e., the beam has the maximum area. It is more easy to understand this fact if one imagines the dividing of the beam incident on the side  $G_1$  into two equal beams 1 and 2 and to follow their traces inside the crystal separately. The middle beam passes through the middle of the side  $G_1$  in all three cases shown in Fig. 4, and occurs at the border of the side  $G_2$  after the internal reflections. The extreme beams incident on  $G_1$  occur at the middle of the side  $G_2$ . The dotted vertical lines in the middle of the figure divide the bases into three equal parts, and into five parts in the lower figure.

In contrast to the beams "a," the cross sections of which are always greater than zero, the beams "b" can have zero cross section. Three processes are shown in Fig. 5, when all beams outgoing from the side  $G_1$  propagate along the direction of the externally reflected beam. The extreme beams incident on  $G_1$  occur at the border of the side  $G_2$  in all three cases. The dotted vertical lines of the figure divide the bases into two equal parts, and into three parts in the lower figure.

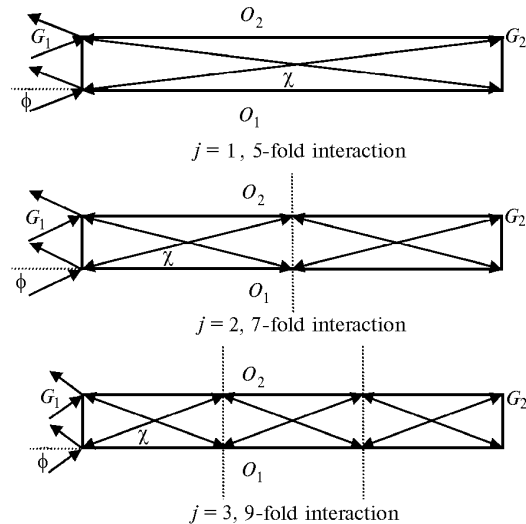


**Fig. 5.** The diagrams of formation of beams in the hexagonal plates with  $\gamma = 0$ , which are outgoing of the side and give the smallest contribution to the backscattering at a slant incidence of radiation.

One can determine the values of the angles  $\beta_{\max}$ , at which the cross sections of the beams "b" are maximum and the values  $\beta_{\min}$ , when the cross sections of the beams "b" are equal to zero, by the formula

$$\beta(j, g) = \arccos(n/\sqrt{1 + g^2/j^2}), \quad (2)$$

where the half-integer values  $j$  correspond to maxima, and integer ones to minima,  $g = \sqrt{3} a/L$  (the ratio of the bases' lengths to the plate thickness).

In the general case of arbitrary  $\beta$ ,  $a$ , and  $L$  one portion of the beams is outgoing from the particle through the side  $G_1$  in the backward direction, and the other one propagates along the direction of the externally reflected beam. The portion of the beams outgoing backwards is determined by the formula

$$f(\beta, g) = 2 \operatorname{mod}(j(\beta, g), 1) h(t(\beta, g)) + 2 [1 - \operatorname{mod}(j(\beta, g), 1)] h(-t(\beta, g)). \quad (3)$$

Here  $\operatorname{mod}(x, 1)$  is the difference between  $x$  and the neighbor integer to  $x$  so that

$$0 \leq \operatorname{mod}(x, 1) < 1; j(\beta, g) = g \cos\beta/\sqrt{n^2 - \cos^2\beta};$$

$$t(\beta, g) = 1/2 - \operatorname{mod}(j(\beta, g), 1); h(x) = 1/2(1 + |x|/x).$$

The total area of the beams "b" outgoing backwards is calculated by the formula

$$S_b(\beta, a, L) = aL \sin\beta f(\beta, g). \quad (4)$$

The dependences  $S_a(\beta)$  and  $S_b(\beta)$  for the hexagonal plate of the size close to that shown in Fig. 2 ( $a = 200$ ;  $L = 30.64$ ) are shown in Fig. 6 except for the common factor  $aL$ .

The value  $S_a(\beta)$  reaches its maximum at  $\beta \approx 51.2^\circ$ .

The comparison of the behavior of the curves  $M_{11}(0, \beta)$  in Fig. 2 and  $S_b(\beta)$  in Fig. 6 shows entire coincidence of the position of the five right-hand side minima and four maxima on the  $\beta$  axis. The fifth and other maxima are only weakly pronounced. This means that the contribution of the beams "a" to the backscattering prevails on the interval  $0 < \beta < 42^\circ$ . The contribution of the beams "a" and "b" are comparable on the interval  $42 < \beta < 64^\circ$  and the contribution of the beams "b" prevails at  $64 < \beta < 90^\circ$ .

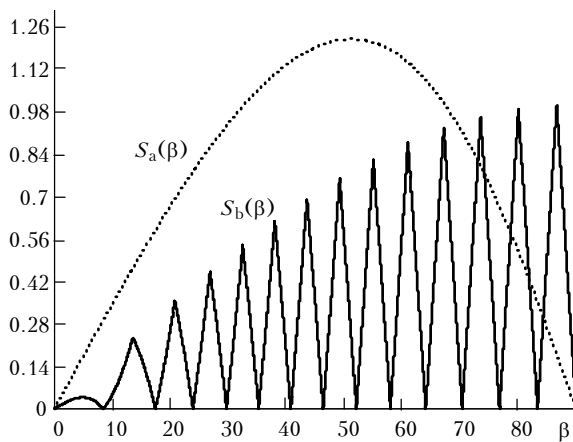


Fig. 6. The dependence of the cross sections of the beams "a" (dotted line) and the beams "b" (solid line) on the angle  $\beta$  for a hexagonal plate.

The function  $M_{11}(0, \beta)$  is shown in Fig. 7 for the hexagonal water ice columns of the diameter  $2a = 131.44 \mu\text{m}$  and the length  $L = 400 \mu\text{m}$ .

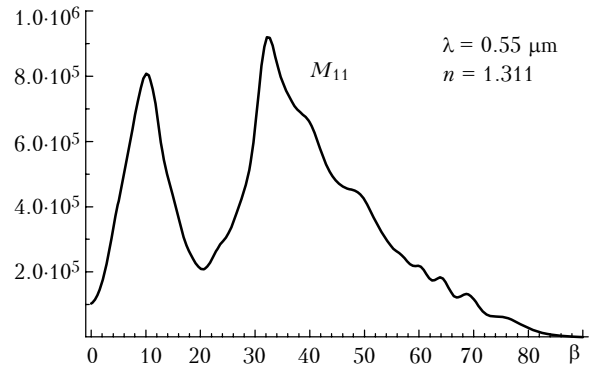


Fig. 7. The function  $M_{11}(0, \beta)$  for the ensemble of hexagonal columns uniformly oriented about the axis.

The aforementioned reasoning for plates can be used for columns, taking into account that in this case the bases and sides change their roles. So the formulas (1)–(4) has the following form for columns:

$$S_a(\beta, a, L) = 2 \sqrt{3} a^2 \cos\beta \sin\beta/\sqrt{n^2 - \cos^2\beta}, \quad (5)$$

$$\beta(j, g) = \arcsin(n/\sqrt{1 + g^2/j^2}), \quad (6)$$

where the half-integer values  $j$  correspond to maxima, and integer ones to minima,  $g = L/\sqrt{3} a$ ;

$$f(\beta, g) = 2 \operatorname{mod}(j(\beta, g), 1) h(t(\beta, g)) + 2 [1 - \operatorname{mod}(j(\beta, g), 1)] h(-t(\beta, g)),$$

$$j(\beta, g) = \frac{g \sin\beta}{\sqrt{n^2 - \sin^2\beta}}, t(\beta, g) = 1/2 - \operatorname{mod}(j(\beta, g), 1),$$

$$h(x) = 1/2(1 + |x|/x); \quad (7)$$

$$S_b(\beta, a, L) = \sqrt{3} a^2 \cos\beta f(\beta, g). \quad (8)$$

The functions  $S_a(\beta)$  and  $S_b(\beta)$  for the hexagonal column of the size analogous to that shown in Fig. 7 ( $a = 65.72$ ;  $L = 400$ ) are shown in Fig. 8 except for the common factor  $\sqrt{3} a^2$ . It is seen that the position of the extreme left-hand side peak in the curve  $S_b(\beta)$  in Fig. 8 coincides with the position of the similar peak in the curve  $M_{11}(0, \beta)$  in Fig. 7, while the second from left peak in  $S_b(\beta)$  practically coincides with the position of the maximum of the curve  $S_a(\beta)$ .

Obviously, at  $g \approx 1$  the maxima from the beams "a" and "b" should coincide. It is confirmed by the behavior of the curve  $\beta(1/2, g)$ , which is the dependence of the position of the first maximum of the contribution of the beams "b" on the ratio between the size of the hexagonal plates  $g$  (Fig. 9). As the contribution of the beams "a" quickly decreases after  $\beta > 58^\circ$ , it is clear that at least one maximum from the beams "b" is displayed starting from  $g > 2$ .

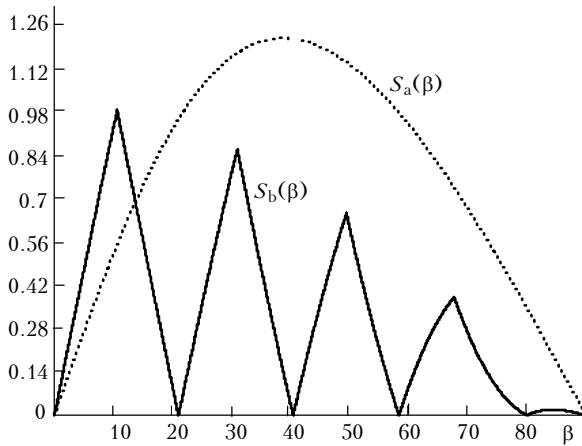


**Fig. 8.** The dependence of the cross sections of the beams "a" (dotted line) and the beams "b" (solid line) on the angle  $\beta$  for a hexagonal column.

Let us note for the conclusion that the aforementioned results significantly differ from that obtained in Ref. 2, where only one maximum in  $M_{11}(\beta)$  was revealed in the interval  $0 < \beta < 90^\circ$ , at  $\beta \approx 32^\circ$ , independently of the relationships between the largest and smallest size of the crystal. Besides, two maxima at  $\beta = 0$  and  $90^\circ$  were noted in Ref. 2, which are significantly lower than that at  $\beta \approx 32^\circ$ .

It has been shown in Ref. 1 that the maximum at  $\beta = 0$  is prevalent for the majority of hexagonal crystals, and the maximum at  $\beta = 90^\circ$  is prevalent only for long columns of small diameter. The results of this paper make an evidence of the fact that one can observe a set of well pronounced extrema in  $M_{11}(\beta)$  as  $\beta$

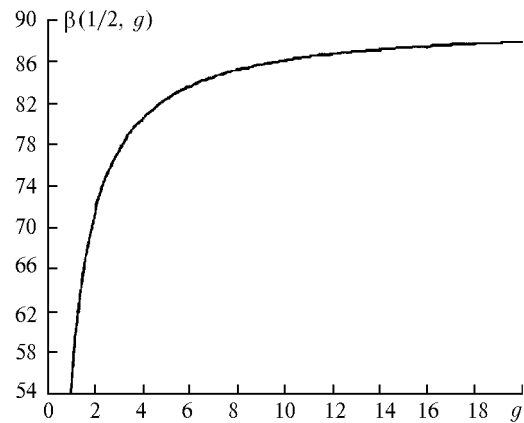


**Fig. 9.** The dependence of the angle  $\beta$ , at which the greatest contribution of the 4-fold beams "b" into the backscattering is observed, on the ratio of the size of hexagonal plates.

changes. The positions of these extrema depend on the ratio between the diameter of the hexagonal crystal and its length.

### Acknowledgments

The work was supported in part by Ministry of Science of Russian Federation (Project "Lidar," No. 06-21).

### References

1. D.N. Romashov, Atmos. Oceanic Opt. **12**, No. 5, 376-384 (1999).
2. E.I. Naats, A.G. Borovoi, and U.G. Ooppel, Proc. SPIE, *Atmospheric and Oceanic Optics*, **3583**, 155-161 (1998).